PENETRATION DEPTH OF DUST GRAINS INTO HIGHLY POROUS PRIMITIVE BODIES. T. Okamoto[1], A. M. Nakamura[1], S. Hasegawa[2], K. Kurosawa[2], K. Ikezaki[3], and A. Tsuchiyama[4], [1]Department of Planetary Sciences, Kobe University, 1-1 Rokkodai, Nada-ku, Kobe, Japan (tokamoto@stu.kobe-u.ac.jp), [2]Institute of Space and Astronautical Science, JAXA, [3]Department of Earth and Space Science, Osaka University, [4]Division of Earth and Planetary Sciences, Kyoto University.

Introduction: Early planetesimals must have been very porous because dust aggregates, the component or the progenitor of planetesimals, are considered to be highly porous [1, 2]. Some of small bodies—such as asteroids, comets, and Kuiper Belt Objects (KBOs)—still have high bulk porosities, up to 86% [3]. As such primitive bodies have been porous throughout the history of the solar system, dust can be captured at the surface of those bodies long after their formation.

Though comets are thought to have been formed in the outer region of the solar system, recent studies have showed that high-temperature products present in comets. Dust particles from comet 81P/Wild2 were found to contain refractory grains such as CAI-like material [4], chondrule-like fragments and chondrule fragments [5, 6]. Meanwhile, spectroscopic observations of both Oort Cloud and Jupiter-family comets found that comets consist of crystalline silicate materials, which are also produced by a high-temperature process [7]. The presence of such high-temperature products in comets suggests that the products formed near the Sun were transported to the formation region of the icy bodies. Grains might have been collected in a debris disk after the bodies formed. In this process, exotic components would have accumulated on the surface of the icy bodies and changed their surface composition.

The purpose of this study is to investigate the penetration depth of dust into small porous bodies. We conducted impact-penetration experiments of millimeter-sized projectiles into highly porous sintered targets [8].

Experiments: We prepared sintered targets characterized by three bulk porosities (94, 87 and 80%; hereafter fluffy94, fluffy87 and fluffy80) using glass beads. Fluffy94 and fluffy 87 were made of hollow soda–lime–borosilicate glass microspheres, with an average diameter and shell thickness of 55 μm, 0.95 μm, respectively, and 2.5 g cm^{-3} in grain density, while fluffy80 were made of low-alkali glass particles of 5 μm in diameter and 2.6 g cm^{-3} in grain density. The typical target lengths and diameters were 130 and 62 mm, respectively, for fluffy94, 100 and 48 mm for fluffy87, and 130 and 62 mm for fluffy80.

Impact experiments were conducted using a two-stage light-gas gun at ISAS, Japan. We used a flash X-ray system to observe the deceleration processes of the projectiles in non-transparent targets. The projectiles were titanium, aluminum, and stainless-steel spheres and basalt cylinders. A cylindrical nylon sabot [9] was used for projectile acceleration. The impact velocities ranged from 1.6 to 7.2 km s^{-1}. The targets' track morphologies and the projectiles' final states were observed on transmission images taken by a micro-X-ray tomography instrument [ELE-SCAN NX-NCP-C80-I (4); Nittetsu Elex Co.] at Osaka University (now at Kyoto) [10].

Results and Discussions: Two types of track morphology were observed [8]. The first type, the carrot-shape, is a thin, long track and occurs when the projectile remains almost intact. The second, the bulb-shape, is thick and short with tails and occurs when the projectile is disrupted. These track types were also observed for dust tracks in silica aerogel [11].

Disruption of the projectiles. Figure 1 shows the relationship of the ratio of the terminal fragment mass, m_L to the initial projectile mass, m_p and the initial dynamic pressure, $\rho_t v_0^2$, where ρ_t and v_0 are the target density and impact velocity, respectively, normalized by the projectile's tensile strength Y_{tp}. Projectile deformation starts at a dynamic pressure of 4–7 times the tensile strength of the projectiles. Projectiles seem to start to lose mass when the dynamic pressure becomes 10 times the projectile tensile strength, and projectiles are then heavily disrupted (terminal-fragment mass fraction < 0.5). The following regression line was obtained for all the data except for the two leftmost points:

$$m_L/m_p = 10^{1.5\pm0.7} \times \left(\frac{\rho_t v_0^2}{Y_{tp}}\right)^{-1.5\pm0.5} . \quad (1)$$

The largest-fragment mass fraction becomes half of the original mass when the dynamic pressure becomes 16 times the projectile tensile strength.

Deceleration of the projectiles. We constructed a simple model for projectile deceleration as follows. When a projectile collides with a target, the projectile loses mass at the impact point because of the high initial pressure. The remaining projectile then penetrates into the target according to the following equation:

$$m_L \frac{dv}{dt} = -\frac{1}{2} C_d \rho_t S_L v^2 - S_L Y_c . \quad (2)$$

where v, C_d, ρ_t, S_L, Y_c are projectile velocity, drag coefficient, target bulk density, cross sectional area of

the terminal projectile, target's compressive strength, respectively. For nearly intact projectile during the penetration, the drag coefficient was determined as 1.1±0.3 in this study and the value was used in this model. The estimated penetration depth is compared with the experimental data in Figure 2. It shows that the estimate reproduces the experimental data well.

We applied this penetration model with the condition for projectile disruption of Eq. 1 to tracks formed by the penetration of silicate dust grains of 2700 kg m^{-3} in density into hypothetical icy bodies of 1600 kg m^{-3} in grain density orbiting in the Kuiper Belt region which were homogeneous on much smaller scales than the impacting dust particles. The result of this calculation is shown in Figure 3. The penetration depth increases with increasing bulk porosity of the target body. For bodies of order 90% bulk porosity, the penetration depth is approximately 100 times the projectile diameter.

References: [1] Suyama, T. et al. (2008) *ApJ, 684,* 1310–1322. [2] Blum, J. and Wurm, G. (2008) *Annu. Rev. Astro. Astrophys. 46,* 21–56. [3] Consolmagno, G. J. et al. (2008) *Chemie der Erde (Geochemistry) 68*, 1–29. [4] Brownlee, D. et al. (2006) *Science 314,* 1711–1716. [5] Nakamura, T. et al. (2008) *Science 321,* 1664–1667. [6] Ogliore, R. C. et al. (2012) *ApJ Letters 745* : L19. [7] Wooden, D. et al. (2007) *Protostars and Planets V. Univ. of Arizona Press, Tuscon,* 815–833. [8] Okamoto, T. et al. (2012) *43rd Lunar and Planetary Science Conference,* abstract #1782. [9] Kawai, N. et al. (2010) *Rev. Sci. Instruments, 81,* 115105. [10] Tsuchiyama, A. et al. (2002) *geochem. J., 36,* 369–390. [11] Hörz, F. et al. (2006) *Science 314*, 1716–1719.

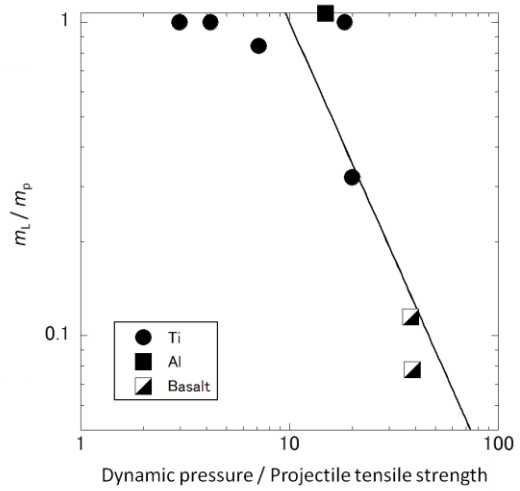

Figure 1. Normalized terminal-fragment mass versus normalized dynamic pressure. The line is a fit to six data points for deformed or disrupted projectiles with dynamic pressure / projectile tensile strength > 6.

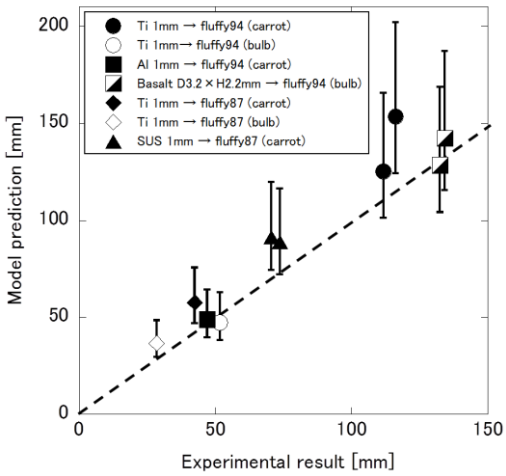

Figure 2. Comparison of the estimated penetration depth and the experimental results. The dashed line shows a reference where both are in agreement.

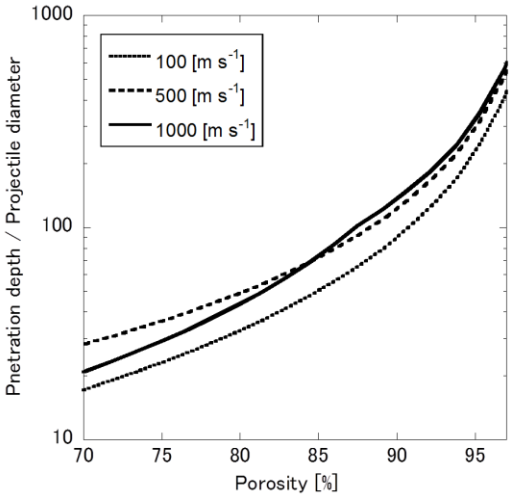

Figure 3. The estimated penetration depth at each impact velocity versus the bulk porosity of the icy bodies, which are homogeneous on a much smaller scale than the impacting dust particles.

Acknowledgments: We are grateful to the Space Plasma Laboratory, ISAS, JAXA, Japan for support of our experiment.